# AC voltage comparison of the Josephson Voltage Standards of the PTB and the BIPM

**(part of the ongoing BIPM key comparison BIPM.EM-K10.c and d)[1]**

S. Solve*, R. Chayramy*, M. Stock*, L. Palafox** and R. Behr**

*Bureau International des Poids et Mesures
F- 92312 Sèvres Cedex, France

**Physikalisch-Technische Bundesanstalt
Bundesallee 100
D-38116 Braunschweig, Germany

**Abstract.** A comparison of the Root Mean Square (RMS) amplitude of a sinewave (AC signal) generated by a BIPM generator was performed between the *Bureau International des Poids et Mesures* (BIPM) and the *Physikalisch-Technische Bundesanstalt* (PTB). The AC signal was measured alternatively by Josephson array voltage standards of the BIPM and the PTB in the PTB laboratory in Braunschweig, Germany. The comparison was carried out in June 2025 at RMS voltages of 0.75 V and 7 V at different frequencies in the range from 62.5 Hz to 1250 Hz. This key comparison is the first official exercise since the revision of the BIPM.EM-K10 comparison protocol[1], endorsed by the Consultative Committee for Electricity and Magnetism (CCEM) in June 2022. In the present case, only the option IV of the technical protocol was followed. The final results were in very good agreement of a few parts in $10^8$ V $V^{-1}$ at both nominal voltages.

## 1. Introduction

Within the framework of CIPM MRA key comparisons, the *Bureau International des Poids et Mesures* (BIPM) and the *Physikalisch-Technische Bundesanstalt* (PTB) performed an on-site comparison of the Root Mean Square (RMS) amplitude of a sinewave (AC signal) generated by a

[1] In addition to DC comparisons: *.a* for 1 V and *.b* for 10 V, BIPM.EM-K10 offers 2 new extensions: *.c* for 0.75 V RMS and *.d* for 7 V RMS

BIPM generator operated as a transfer standard in Braunschweig, Germany, in June 2025. This exercise is the first of this type and follows the new protocol of BIPM.EM-K10, extended to AC voltages, which was endorsed by the Consultative Committee for Electricity and Magnetism (CCEM) in June 2022 [1]. The transfer standard was measured alternatively by the BIPM transportable programmable Josephson voltage standard (PJVS) and associated measurement setup and that of the PTB, using the differential sampling technique [2].

The BIPM PJVS was shipped to PTB, Germany, where an on-site direct comparison was carried out from 16 June to 27 June 2025. The present comparison followed the technical rules of option IV of the BIPM.EM-K10 comparison protocol.

This comparison option involved the BIPM transportable PJVS and the PTB Quantum Voltmeter [4, 5] to measure the RMS value of sinewaves generated by the BIPM transfer standard consisting of a Signal Waveform Generator (SWG) generator and filter [3] using the differential sampling technique. The transfer standard was alternatively measured by the BIPM PJVS and the PTB Quantum Voltmeter following the sequence ABBA where A stands for PTB and B for BIPM. The results are expressed as the relative mean values: $(U_{PTB} - U_{BIPM}) / U_{BIPM}$ in parts in $10^8$.

This article describes the technical details and the results of the experiments carried out during the comparison.

## 2. Comparison equipment

### *2.1 The BIPM AC quantum voltmeter*

The BIPM programmable Josephson voltage standard (PJVS) is composed of a cryoprobe that carries a liquid-helium version of the 2 V or 10 V SNS NIST programmable array [6-10]. The 2 V array was operated for the measurements at 0.75 V RMS to limit the leakage error to ground and the 10 V array was used at the 7 V RMS level. The voltage across the array is controlled by a dedicated microwave source and a dedicated current bias source. The array must be cooled down in a bath of liquid He. The PJVS was operated with the *Supracon* bias source and associated software [11] at 0.75 V RMS and with the NIST bias source (JVS-650) and associated software (iPJVS Core 2021-v1208) at 7 V RMS. The 2 V programmable array contains 61204 Josephson junctions (double stacked) with a critical current of 10.5 mA [6], while the 10 V array has 265116 Josephson junctions (triple stacked) with a critical current of 7 mA [7]. The system uses a programmable 18 GHz to 20 GHz microwave synthesizer to frequency-bias the PJVS arrays [8]. The microwave power is set to about 40 mW for optimum step widths of the 2 V array and 100 mW

for the 10 V array. When biasing all segments of the 2 V and 10 V arrays, the measured quantum locking ranges are, respectively 2.5 mA and 1.1 mA.

The BIPM traveling quantum voltage standard is flexible and is optimized to limit the errors introduced by the electromagnetic environment of the participant's laboratory and possible systematic errors and noise due to grounding effects and/or AC capacitive coupling effects. The PJVS is electrically floating with no connection to earth potential, but its low potential side can be grounded whenever necessary. The series resistance of each of the precision measurement leads is 2.5 Ω, and their leakage resistance to earth is 80 GΩ. These values were checked on-site using a dedicated feature of the iPJVS Core software. However, the AC component, i.e. capacitive component of the leakage impedance cannot be measured easily. This component increases the leakage error as the frequency of the measured signal rises. The value of the thermal electromotive forces (EMFs) measured at the level of the output connection (at the laboratory temperature) is in the range 600-900 nV. For the AC voltage comparison, the setup is flexible and allows a large number of possibilities for differential sampling, among which the principal ones are:

- 2 V array instead of 10 V array to limit the number of cells connected to the array and corresponding leakage paths to ground.
- The BIPM differential sampling setups can operate three different samplers. During this comparison only the NI PXI-5922 was used. The sampler is inserted into a NI-PXI 1031DC chassis powered by an isolated supply and PC-controlled via an optical link.
- The BIPM setup can be operated with different software. For convenience, the PTB software was operated on both differential sampling computers (BIPM and PTB).

### *2.2 The PTB AC quantum voltmeter*

The PTB AC quantum voltmeter that was operated during the comparison uses a commercially available NPL bias source [12] to drive either a 2 V or a 10 V array. The 2 V programmable array contains 16384 (8192 double-stacked) Josephson junctions with a critical current of 3.2 mA while the 10 V array has 69632 Josephson junctions with 5.2 mA critical current [13]. The system uses a programmable 70 GHz microwave synthesizer to drive the arrays [14]. The microwave power is set to about 50 mW for optimum step widths of the 2 V array and 100 mW for the 10 V array. Operating margins are 2 mA and 0.8 mA wide for the 2 V and 10 V array, respectively. After setting the array bias currents, the system can be operated for weeks without re-adjusting the parameter settings. No parameter changes were required for the duration of the measurements presented in this paper.

The system is electrically insulated, and the computer is connected via an optical ring [15]. Each of the segments in the binary divided Josephson array is driven by a separate channel of the bias source. The channels have an amplitude resolution of 14 bits and the transitions at the output of the arrays show transient times below 300 ns.

- The AC quantum voltmeter uses an isolated power supply to run a ΣΔ-analogue-to-digital converter (ΣΔ-ADC) as sampler. Hence the whole AC-QVM is electrically isolated. The trigger and clock signals, which are optically isolated, are generated by two synthesizers locked to the 10 MHz reference to synchronize the ΣΔ-ADC and the PJVS bias source. A waveform generator (Keithley 3390) is used to set the phase shift between the SWG waveform and the AC-QVM stepwise approximated sine wave. The precise phase adjustment is performed manually by de-tuning the 20 MHz clock optically fed to the NPL source until the RMS value of the difference at the ΣΔ-ADC reaches the lowest signal amplitude, which is achieved when the sine wave crosses precisely the centers of the PJVS steps. We selected the NI PXI 5922 card for our measurements and operated it in the 10 $V_{p-p}$ range at 4 MSa $s^{-1}$ and 10 MSa $s^{-1}$ sample rates [16]. The card was operated in an NI-PXI 1038DC chassis controlled from a PC using an optical link.

## 3. Comparison procedure - Option IV

### *3.1 Introduction*

Option IV of the comparison protocol has been designed to achieve the lowest voltage difference and corresponding Type A uncertainty between the participants.

The 10 MHz reference signal distributed in the PTB laboratory is used by both setups. In order to avoid any interference, the signal is decoupled between the two setups using isolation transformers.

In option IV, the transfer standard is an AC source and associated output filter provided by the BIPM (commercial AC source designed and assembled at CMI - Czech Metrology Institute) [3].

A computer-controlled switch (BNC connectors type) was installed on the BIPM transfer standard in order to easily switch its output between the BIPM measurement setup and the PTB measurement setup and to reduce the connection time to the minimum possible. Furthermore, any physical manipulations and related possible changes between the two measurement setups are avoided.

The voltage difference between the two participants is evaluated from a series of individual measurements (typically 5 to 10) performed by each participant following an ABBA sequence,

where A stands for the PTB and B for the BIPM. More details on this measurement acquisition process are given on the next paragraph.

### *3.2 Measurement precautions and improvements*

After the BIPM JVS was set up, the array of Josephson junctions was checked for trapped flux.
Before we carried out comparisons, the following preparations were made:

1) Both Josephson systems were connected to the same power strip.

2) The earthing point, which was used in a star configuration for all earthing, was located on this power strip.

3) This configuration provided the best results in the pilot studies and was therefore never changed.

4) Both PJVS systems used a single 10 MHz reference for timing and RF bias provided by PTB.

5) The 10 MHz connections to the *Supracon* bias source and its trigger output were additionally insulated (Fig. 1).

6) The stepwise approximated sinewave of the BIPM PJVS was synchronized to an external signal: Waveform Generator (WG) feeding the 10 MHz to the *Supracon* bias source at 0.75 V RMS and SWG Trig out signal feeding the NIST bias source at 7 V RMS.

7) The SWG BIPM Transfer Standard and associated filter were operated on batteries and an external battery pack connected to each device ensured long term operation.

8) The RF line to the NIST array was provided with an additional DC block at 0.75 V RMS even if explicit evidence of improvements couldn't be found.

### *3.3 Measurement setup*

The measurement loop operated for the option IV comparison is based on the synchronization of the two AC quantum voltmeters with the SWG synthesizer. A schematic of the set-up and the synchronization is shown in figures 1 and 2, reflecting the different setups used at 0.75 V and 7 V. The computer-controlled switch provides the capability to physically connect both measurement setups to the SWG.

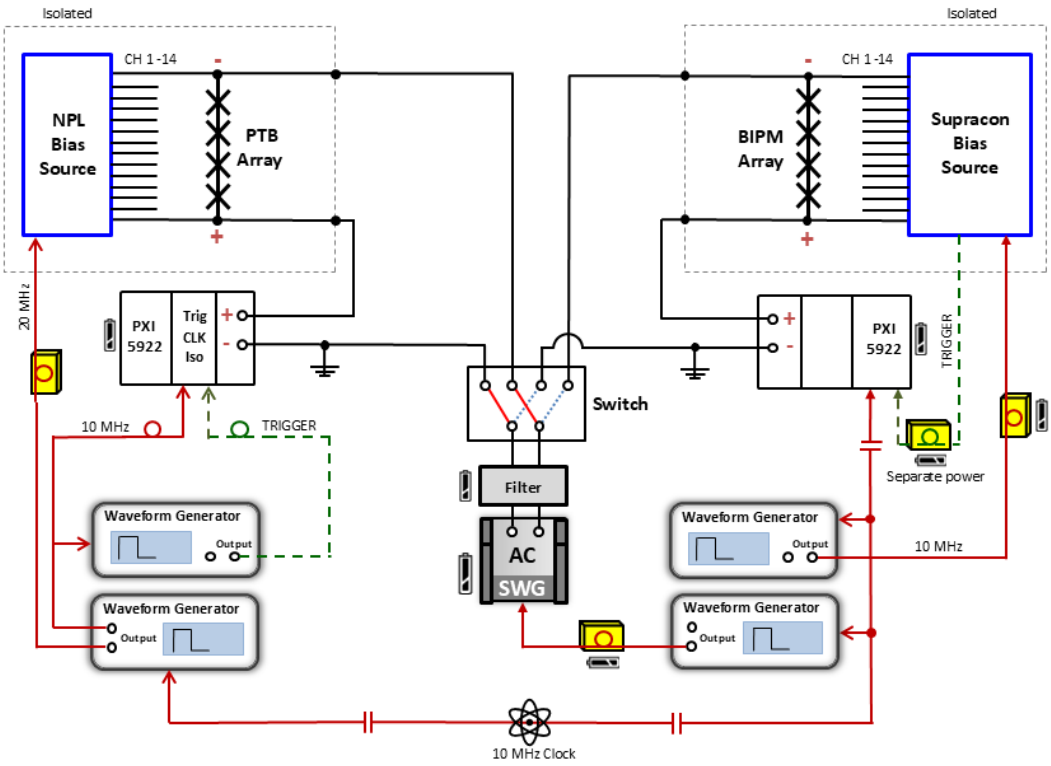


**Fig. 1:** Measurement setup used for the 0.75 V RMS comparison including synchronization scheme. Red lines show 10 MHz distribution and green dashed lines trigger connections. Optical isolators are indicated by loops on the connections.

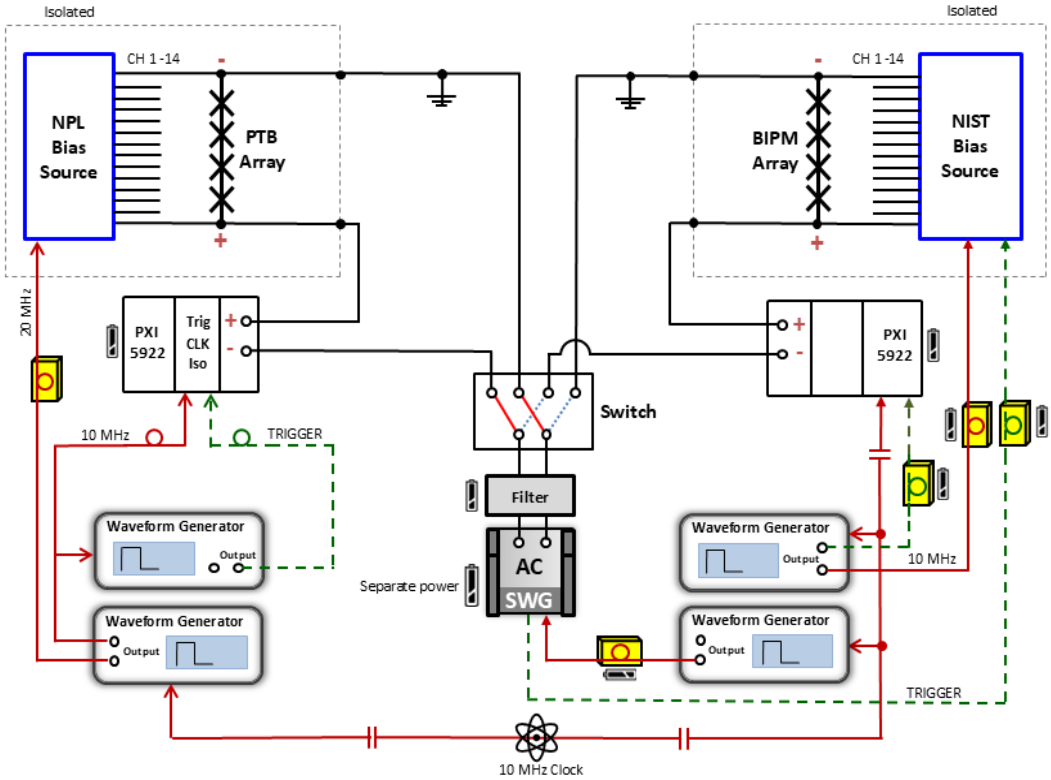


**Fig 2**: Measurement setup used for the 7 V RMS comparison including synchronization scheme. Red lines show 10 MHz distribution and green dashed lines trigger connections. Optical isolators are indicated by loops on the connections.

### *3.4 ABBA procedure*

Once the two systems had been synchronised with the SWG, the measurements of the output voltage of the SWG could be carried out in quick succession. An Allan analysis showed that the measurement of the output voltage of the SWG reached the uncertainty range of $10^{-8}$ V $V^{-1}$ after around 60 seconds for all frequencies and should therefore be measured in this way. Switching from one system to the other only took about 10 seconds. This means that an ABBA measurement took about 5 minutes and the series of 5 ABBAs about 30 minutes. Due to the fast switching between the two Josephson systems without the need for further adjustment steps, the drift of the SWG, although typically less than $1 \times 10^{-7}$ V $V^{-1}$ over 30 minutes, could be tracked very well. This reduced the Type A measurement uncertainty. Some examples of such measurement series are shown in the appendix.

### *3.5 Grounding*

The earthing concept is based on the optimised strategy developed in the pilot studies. It consists of a central potential reference point (Earth of the PTB laboratory) designated as “star point”. All the chassis of the instrumentation, shields of cables, helium dewars and:

- the low potential of the arrays when the sampler is installed between the high potential of the PJVSs and the AC source (e.g. see Fig. 2),
- the low potential of the sampler (NI-5922) when the sampler is installed between the high potential of the PJVSs and the low potential of the AC source (e.g. see Fig. 1),

are referred to this unique potential reference point.

### *3.6 Trapped flux*

During the time of the comparison, it was regularly checked whether either of the two AC quantum voltmeters had trapped flux. This could also be done quickly and easily during the measurements by varying the microwave power. If one of the Josephson systems had trapped flux, the measurement voltage easily followed the microwave power.

## 4. Comparison results - Option IV at the 0.75 V and 7 V level

### *4.1 Measurements at 0.75 V*

On 17 June we carried out five ABBA measurement points for the frequencies 62.5 Hz, 125 Hz, 312.5 Hz, 625 Hz, and 1000 Hz. On 18 June we repeated two ABBA series at 625 Hz and one at 1000 Hz. Series at the same frequency are averaged. The readings of the sampler were evaluated by using an Allan variation analysis. Typically, the measurement uncertainty determined in this way was on the order of a few parts in $10^8$ (see the appendix for some examples). In figure 3 and

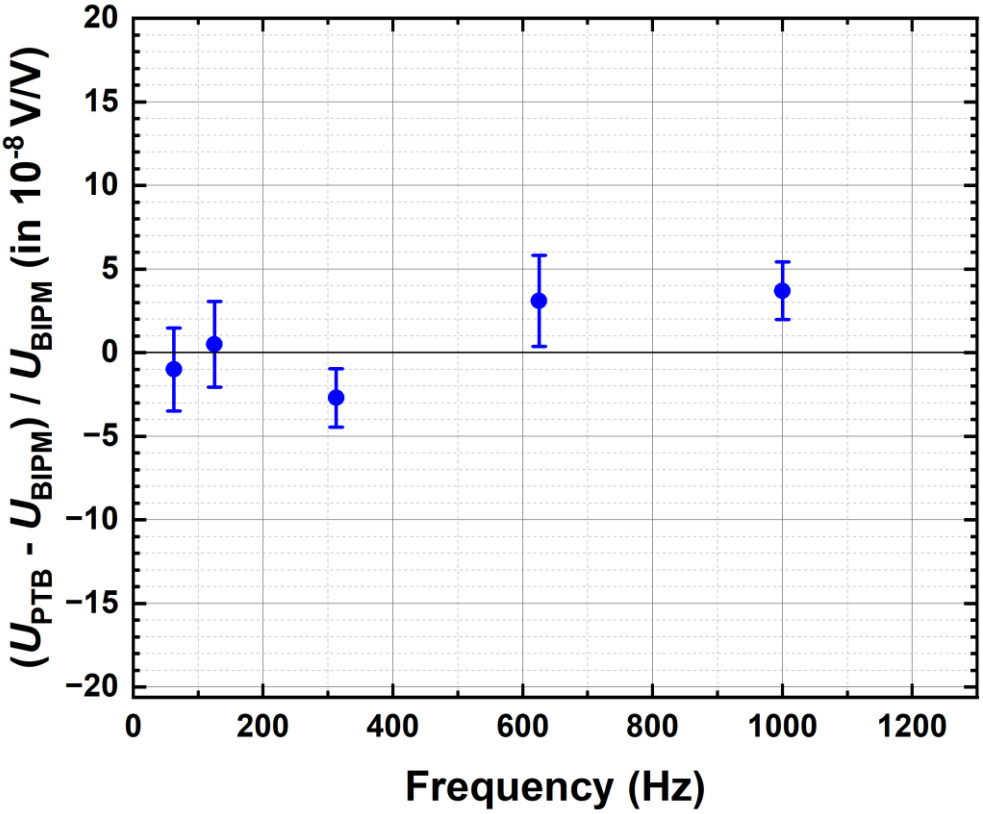


**Fig. 3**: Individual results obtained at 0.75 V for frequencies from 62.5 Hz to 1 kHz. The error bars indicate the total uncertainty of the measurements for $k = 1$.

table 1 the mean comparison values $(U_{PTB} - U_{BIPM}) / U_{BIPM}$ are presented. The error bars indicate the total uncertainty of the measurements for $k = 1$. For the Type B uncertainty evaluation see chapter 5.

**Table 1**: Final results for the comparison at 0.75 V RMS.

| Frequency / Hz | 62.5 | 125 | 312.5 | 625 | 1000 | 1250 |
|---|---|---|---|---|---|---|
| $(U_{PTB} - U_{BIPM}) / U_{BIPM}$ (in $10^{-8}$ V $V^{-1}$) | -1.0 | 0.5 | -2.7 | 3.1 | 3.7 | - |
| Relative Total Combined Uncertainty (in $10^{-8}$ V $V^{-1}$) | 2.5 | 2.6 | 1.7 | 2.7 | 1.7 | - |

On 18 and 19 June the first Type B uncertainty evaluations were performed. Attempts were then made on the following days to further improve the comparison results. Since small changes from the optimal measurement setup can lead to interferences, the results were rarely reproducible and are not discussed further here.

### *4.2 Measurements at 7 V*

On 27 June we carried out eight ABBA measurement points for the frequencies 62.5 Hz, 125 Hz, 312.5 Hz, 625 Hz (2x), 976.5625 Hz, 1000 Hz, and 1250 Hz with the setup shown in Fig. 2. In figure 4 and in table 2 the mean comparison values $(U_{PTB} - U_{BIPM}) / U_{BIPM}$ are presented. The error bars indicate the total uncertainty of the measurements for $k = 1$. For the Type B uncertainty evaluation see chapter 5.

**Table 2**: Final results for the comparison at 7 V RMS.

| Frequency / Hz | 62.5 | 125 | 312.5 | 625 | 976.5625 | 1000 | 1250 |
|---|---|---|---|---|---|---|---|
| $(U_{PTB} - U_{BIPM}) / U_{BIPM}$ (in $10^{-8}$ V $V^{-1}$) | -2.6 | -3.0 | -5.4 | -4.4 | 4.3 | 2.4 | 16.4 |
| Relative Total Combined Uncertainty (in $10^{-8}$ V $V^{-1}$) | 2.7 | 2.7 | 2.6 | 2.7 | 3.4 | 3.3 | 4.0 |

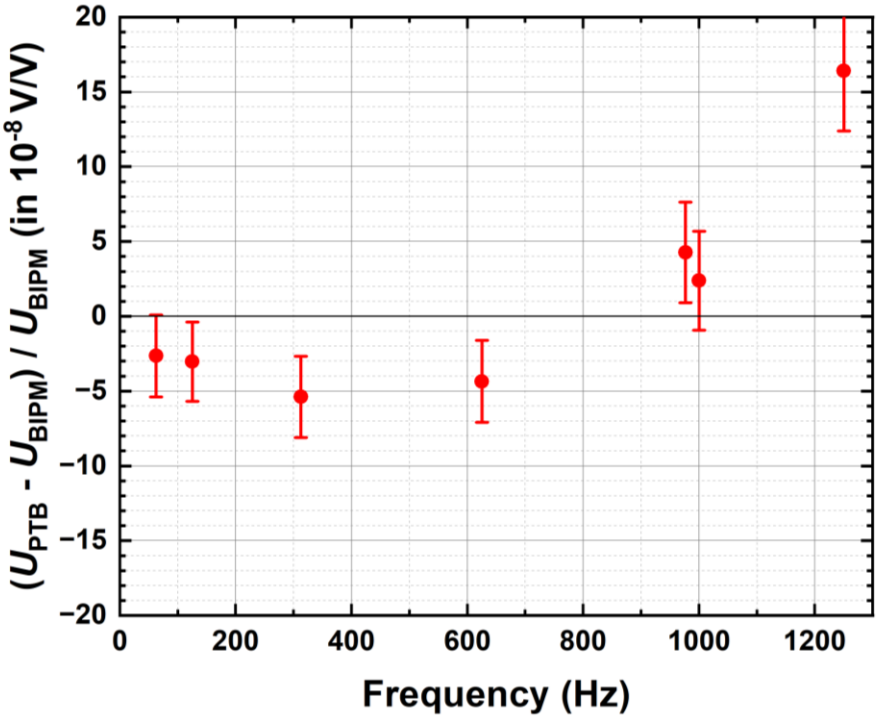


**Fig. 4**: Individual results obtained at 7 V for frequencies from 62.5 Hz to 1.25 kHz. The error bars indicate the total uncertainty of the measurements for $k = 1$.

## 5. Evaluation of the Type B uncertainty components

The sources of Type B uncertainty for 0.75 V and 7 V at 1 kHz (Tables 3 and 4 respectively) are: the frequency accuracy of the BIPM and the PTB microwave synthesizers, the leakage currents, the sampler gains and filters, the cable errors, and the switch. Frequency uncertainty and leakage resistance which are relevant for DC Josephson voltage standards are only shown for the sake of completeness. They are negligible for the AC comparison, as are the thermal voltages, typically only a few 100 nV. These contribute quadratically to the effective value of the measured voltage, result normally in less than $10^{-12}$ V and are therefore negligible. Most of the effects of sampler noise and gain stability are already contained in the Type A uncertainty. The effect of electromagnetic interferences is also contained in the Type A uncertainty. Uncertainty components related to RF power rectification and sloped Shapiro voltage steps are considered negligible because no such behaviour was observed. The drift of the BIPM SWG transfer standard was followed by each measurement setup and therefore is also part of the Type A uncertainty.

| | Type | Relative uncertainty at 0.75 V and 1 kHz in V $V^{-1}$ | |
|---|---|---|---|
| | | **BIPM** | **PTB** |
| Frequency offset (A) | B | $3.2 \times 10^{-12}$ | $4.0 \times 10^{-12}$ |
| Leakage resistance (B) | B | $1.8 \times 10^{-11}$ | $8.0 \times 10^{-12}$ |
| Sampler Filter (C) | B | 0 | |
| Sampler Gain (D) | B | $0.5 \times 10^{-8}$ | $1.0 \times 10^{-8}$ |
| Cable error (E) | B | $0.2 \times 10^{-8}$ | |
| Switch (F) | B | $1.2 \times 10^{-8}$ | |
| CMRR (G) | B | - | |
| **Total combined Type B** | | **$1.6 \times 10^{-8}$** | |

**Table 3:** Estimated Type B relative standard uncertainty components at 0.75 V and 1 kHz.

| | Type | Relative uncertainty at 7 V and 1 kHz in V V$^{-1}$ | |
|---|---|---|---|
| | | **BIPM** | **PTB** |
| Frequency offset [A] | B | $3.2 \times 10^{-12}$ | $4.0 \times 10^{-12}$ |
| Leakage resistance [B] | B | $1.8 \times 10^{-11}$ | $8.0 \times 10^{-12}$ |
| Sampler Filter [C] | B | 0 | |
| Sampler Gain [D] | B | $1.0 \times 10^{-8}$ | $2.0 \times 10^{-8}$ |
| Cable error [E] | B | $0.2 \times 10^{-8}$ | |
| Switch [F] | B | $1.2 \times 10^{-8}$ | |
| CMRR [G] | B | $2.2 \times 10^{-8}$ | |
| **Total combined Type B** | | **$3.3 \times 10^{-8}$** | |

**Table 4:** Estimated Type B relative standard uncertainty components at 7 V and 1 kHz.

[A] As both systems were locked to the same 10 MHz frequency reference, only Type B uncertainties from the frequencies of the two RF synthesizers are included. The 10 MHz signal used as the frequency reference for the comparison was produced by PTB's atomic clock.
The relative frequency uncertainty for the offset of the frequency of the BIPM PJVS, estimated as 0.1 Hz, can be calculated from the formula: $u = (1/\sqrt{3}) \times (0.1/18) \times 10^{-9} = 3.2 \times 10^{-12}$ V V$^{-1}$.
For the compact PTB microwave synthesizer a comparison with another synthesizer has been performed and the relative frequency offset between them was measured to be less than $4 \times 10^{-12}$ V V$^{-1}$ [17].

[B] If a rectangular statistical distribution is assumed then the relative uncertainty contribution of the leakage resistance $R_L$ can be calculated as: $u = (1/\sqrt{3}) \times (r / R_L)$, with $r$ being the resistance of the measurement leads. For PTB, the related variables are $r = 2.8\ \Omega$ and $R_L = 2 \times 10^{11}\ \Omega$. The isolation resistance value includes all the cables from the JVS to the DVM. For BIPM, those parameters are measured as $r = 2.5\ \Omega$ and $R_L = 8 \times 10^{10}\ \Omega$ [17].

[C] The error due to the digital filter of the NI PXI 5922 has been investigated and published in previous papers [18-19]. To minimize the error due to different filter functions as much as possible both samplers were set to the same sampling rates of 10 MSa s$^{-1}$ for all frequencies above 62.5 Hz and 4 MSa s$^{-1}$ at 62.5 Hz always using the "48-tap standard" finite-impulse-response

digital filter. After this measure, we assume that small errors at these low frequencies can be completely neglected.

(D) The sampler gain was usually calibrated before each new ABBA measurement series using an approximated triangle waveform generated by each PJVS covering the maximum voltage difference measured by the sampler. The PJVS peak amplitude was set to 150 mV (for 0.75 V) and 1 V (for 7 V), the expected amplitudes at the sampler in the differential measurement. Then, for differential sampling the PJVS peak amplitude was set to 1.0606 V (for 0.75 V RMS), we synchronized the two systems and measured the SWG RMS amplitude with the AC-QVM. Each measurement point was adjusted by its corresponding gain and offset values.
The software used to reconstruct the waveform at the input of the AC-QVM includes the gain of the sampler as a parameter. We deliberately changed the gain in the software by $\pm 500 \times 10^{-6}$ and $\pm 1000 \times 10^{-6}$. The corresponding changes in the amplitude are suppressed for differential sampling with 20 Josephson steps by a factor of 348.3 (BIPM) and 348.5 (PTB).
We recorded the gain change between measurement series. On 17 and 18 June we recorded 6 times gain changes at 0.75 V with an averaged change of $\pm$ 3.5 µV $V^{-1}$ and $\pm$ 1.7 µV $V^{-1}$during the measurement sequences for PTB's and BIPM's sampler, respectively. For a Gaussian distribution the relative uncertainties $u_G$ = 3.5 µV $V^{-1}$ / 348.5 = $1.0 \times 10^{-8}$ V $V^{-1}$ ($k$ = 1) and $u_G$ = 1.7 µV $V^{-1}$ / 348.3 = $5.0 \times 10^{-9}$ V $V^{-1}$ ($k$ = 1).
On 27 June the gains of the samplers were calibrated before the start of eight ABBA series at 7 V, performed in rapid succession. Because the gain factors were not calibrated in between, we estimate the error to be twice as large as for the uncertainty at 0.75 V. This corresponds to the typical variation of the gain factor during the two-week measurements.

(E) The Josephson voltages are only quantised on the chip. Due to the long output cables, the AC voltages at the input of the sampler have an error. In addition, the current source also has an influence on the cable error. At 1 kHz, the relative error is approximately 3 x $10^{-8}$ V $V^{-1}$ [18]. As the BIPM and PTB Josephson voltage standards use approximately the same cable lengths but different cables, only the difference between the two cable errors needs to be considered for the comparison. This error was analysed experimentally. For this purpose, the cable lengths were extended by 1 m and 2 m on both sides. These changes only led to very small changes of the measured voltage differences. From this it can be concluded that the cable errors of both AC quantum voltmeters are very similar. Because cable lengths contribute quadratically to the error, a quadratic fit can describe the deviations with cable extensions. This makes it possible to estimate

the error due to the cables actually used in the comparison. A description and an illustration are shown in the appendix. The cable error is estimated to $0.2 \times 10^{-8}$ V V$^{-1}$ ($k$ = 1).

(F) The contribution from the switch was evaluated experimentally by performing two consecutive measurements immediately before and after interchanging the inputs used by the PJVS systems. The differences between *Forward* and *Reversed* measurements were $-0.7 \times 10^{-8}$ V and $3.2 \times 10^{-8}$ V for the BIPM and PTB, respectively. The measurements are shown in the appendix. From this, we evaluate the measurement relative uncertainty for the switch as

$$((3.2 - 0.7) / 2) \times 10^{-8} \text{ V} / \sqrt{2} / 0.75 \text{ V} = 1.2 \times 10^{-8} \text{ V V}^{-1} \ (k = 1).$$

(G) For the measurements at 7 V, both Josephson arrays were connected to earth potential directly and the samplers were operated between the 'high' connections. The common mode rejection ratio (CMRR) of the sampler contributes to the measured value. As the two systems were using the same model of sampler with the same power supply arrangements and used similar sampling parameters, only the difference in CMRR between the two samplers employed affects the result of the comparison. A more detailed description is given in the appendix. The error is frequency-dependent and is calculated at 1 kHz as $2.2 \times 10^{-8}$ V V$^{-1}$ ($k$ = 1). This becomes the dominant contribution and, for future comparisons that use this configuration, we recommend measuring the CMRR of both samplers instead of estimating a difference of 10 % between the two samplers.

For the option IV comparison protocol, the total combined Type B uncertainty comprises all the BIPM Type B components to which the PTB Type B uncertainties are combined quadratically:

$u_B / U_{BIPM} = 1.6 \times 10^{-8}$ V V$^{-1}$ at 0.75 V, $u_B / U_{BIPM} = 2.6 \times 10^{-8}$ V V$^{-1}$ at 7 V for 62.5 Hz and

$u_B / U_{BIPM} = 1.6 \times 10^{-8}$ V V$^{-1}$ at 0.75 V, $u_B / U_{BIPM} = 3.3 \times 10^{-8}$ V V$^{-1}$ at 7 V 1 kHz.

## 6. Conclusion

The comparison was carried out in the PTB Electricity Laboratories in Braunschweig where the environmental conditions allowed meeting good conditions for the stability of the quantum voltages. The PTB AC quantum voltmeter was compared to the BIPM quantum voltage standard. This is the first comparison of its kind since the BIPM.EM-K10 comparison protocol has been revised and extended to AC voltages using the differential sampling technique. Despite several pilot studies performed in preparation it is a difficult exercise in particular because of the introduction of several possible systematic errors [20, 21]. For example, it was not easy to avoid

interferences caused by small imperfections in the measurement setup. These interferences can lead to significant deviations on the order of a few $10^{-7}$ V $V^{-1}$.

Further investigations should be carried out in this field, especially on the determination of the Type B uncertainties, and particularly the capacitive component of the leakage impedance to ground. The electromagnetic compatibility of the participant laboratory as well as the quality of the mains power have also a strong impact on the quality of the measurements and are very difficult to quantify.

Despite these main difficulties, the BIPM PJVS traveling standard and PTB Quantum Voltmeter were successfully compared, with a relative agreement of a few parts in $10^8$ V $V^{-1}$ for both voltages (0.75 V RMS and 7 V RMS) at different frequencies ranging from 62.5 Hz to 1250 Hz. The final results are reminded below:

Degrees of equivalence of the comparison at 0.75 V RMS.

| Frequency / Hz | 62.5 | 125 | 312.5 | 625 | 1000 | 1250 |
|---|---|---|---|---|---|---|
| $(U_{PTB} - U_{BIPM}) / U_{BIPM}$ (in $10^{-8}$ V $V^{-1}$) | -1.0 | 0.5 | -2.7 | 3.1 | 3.7 | - |
| Relative Total Combined Uncertainty (in $10^{-8}$ V $V^{-1}$) | 2.5 | 2.6 | 1.7 | 2.7 | 1.7 | - |

Degrees of equivalence of the comparison at 7 V RMS.

| Frequency / Hz | 62.5 | 125 | 312.5 | 625 | 976.5625 | 1000 | 1250 |
|---|---|---|---|---|---|---|---|
| $(U_{PTB} - U_{BIPM}) / U_{BIPM}$ (in $10^{-8}$ V $V^{-1}$) | -2.6 | -3.0 | -5.4 | -4.4 | 4.3 | 2.4 | 16.4 |
| Relative Total Combined Uncertainty (in $10^{-8}$ V $V^{-1}$) | 2.7 | 2.7 | 2.6 | 2.7 | 3.4 | 3.3 | 4.0 |

## Acknowledgement

We thank Jan Kučera (CMI) and Jakub Kováč for providing the SWG filter and constant support.

## References


[1] Solve S 2023 On-site comparison of dc and ac voltages from Josephson arrays, Technical Protocol for BIPM.EM-K10 comparisons, BIPM KCDB, https://www.bipm.org/kcdb/comparison?id=1779

[2] Behr R, Palafox L, Ramm G, Moser H, and Melcher J 2007 Direct comparison of Josephson waveforms using an AC quantum voltmeter *IEEE Transactions on Instrumentation and Measurement* 56 pp 235–8, https://doi.org/10.1109/TIM.2007.891076

[3] Kučera J, Kováč J, Palafox L, Behr R and Vojáčková L 2020 Characterization of a precision modular sinewave generator *Measurement Science and Technology* 31 pp 064002, https://dx.doi.org/10.1088/1361-6501/ab6f2e

[4] Rüfenacht A, Burroughs C J, Dresselhaus P D, and Benz S P 2013 Differential sampling measurement of a 7 V RMS sine wave with a programmable Josephson voltage standard *IEEE Transactions on Instrumentation and Measurement* 62 pp 1587–93, https://doi.org/10.1109/TIM.2013.2237993

[5] Lee J, Behr R, Palafox L, Katkov A, Schubert M, Starkloff M and Böck A C 2013 An AC quantum voltmeter based on a 10 V programmable Josephson array *Metrologia* 50 pp 612–22, https://doi.org/10.1088/0026-1394/50/6/612

[6] A. Rufenacht *et al.*, "Simultaneous double waveform synthesis with a single programmable Josephson voltage standard," in *2016 Conference on Precision Electromagnetic Measurements (CPEM 2016)*, IEEE, Jul. 2016, pp. 1–2, https://doi.org/10.1109/CPEM.2016.7540471.

[7] Y. Tang et al., "A 10 V programmable Josephson voltage standard and its applications for voltage metrology," Metrologia, vol. 49, no. 6, pp. 635–643, Dec. 2012, https://doi.org/10.1088/0026-1394/49/6/635.

[8] A. Rüfenacht, N. E. Flowers-Jacobs, and S. P. Benz, "Impact of the latest generation of Josephson voltage standards in ac and dc electric metrology," *Metrologia*, vol. 55, no. 5, pp. S152–S173, Oct. 2018, https://doi.org/10.1088/1681-7575/aad41a.

[9] Rufenacht A, Burroughs C J, Benz S P, Dresselhaus P D, Waltrip B C and Nelson T L 2009 Precision Differential Sampling Measurements of Low-Frequency Synthesized Sine Waves With an AC Programmable Josephson Voltage Standard *IEEE Transactions on Instrumentation Measurement* pp 70-1, https://doi.org/10.1109/TIM.2008.2008087

[10] Kim M-S, Cho H, Chayramy R and Solve S 2020 Measurement configurations for differential sampling of AC waveforms based on a programmable Josephson voltage standard: effects of sampler bandwidth on the measurements *Metrologia* 57 065020, https://doi.org/10.1088/1681-7575/aba040

[11] www.supracon.com/de/2020_compact_18channel_bias_source.html

[12] Kleinschmidt P, Patel P D, Williams J M and Janssen T J B M 2002 Investigation of binary Josephson arrays for arbitrary waveform synthesis *IEE Proc.-Sci. Meas. Technol.* 49 313–6

[13] Müller F, Scheller T, Wendisch R, Behr R, Kieler O, Palafox L and Kohlmann J 2013 NbSi barrier junctions tuned for metrological applications up to 70 GHz: 20 V arrays for programmable Josephson voltage standards *IEEE Trans. Appl. Supercond.* 23 1101005, https://doi.org/10.1109/TASC.2012.2235895

[14] Jülicher Squid GmbH, http://www.jsquid.com

[15] Robinson I A 1991 An optical-fiber ring interface bus for precise electrical measurements *Meas. Sci. Technol.* 2 pp 949–56, https://doi.org/10.1088/0957-0233/2/10/011

[16] National Instruments, *NI PXI/PCI-5922 Specifications: Flexible-resolution Digitizer*, Sep. 2018. http://www.ni.com/pdf/manuals/374033b.pdf PXI-5922 Specifications - NI

[17] Solve S, Chayramy R, Stock M, Palafox L and Behr R 2015 Comparison of the Josephson Voltage Standards of the PTB and the BIPM *Metrologia* **52** 01025, https://doi.org/10.1088/0026-1394/52/1A/01025

[18] Behr R and Palafox L 2021 An AC quantum voltmeter for frequencies up to 100 kHz using sub-sampling *Metrologia* 58 025010, https://doi.org/10.1088/1681-7575/abe453

[19] Kim M-S, Cho H, Chayramy R, Solve S 2025 Effect of Sampler Characteristics in Differential Sampling Adopting a Programmable Josephson Voltage Standard *IEEE Transactions on Instrumentation and Measurement* 74 1501507, https://doi.org/10.1109/TIM.2025.3544691

[20] Burroughs C J, Rufenacht A, Benz S P, Dresselhaus P D, Waltrip B C and Nelson T L 2008 Error and Transient Analysis of Stepwise-Approximated Sine Waves Generated by Programmable Josephson Voltage Standards *IEEE Transactions on Instrumentation and Measurement,* https://doi.org/10.1109/TIM.2008.917260

[21] Burroughs C J, Rufenacht A, Benz S P and Dresselhaus P D 2009 Systematic Error Analysis of Stepwise-Approximated AC Waveforms Generated by Programmable Josephson Voltage Standards *IEEE Transactions on Instrumentation Measurement,* https://doi.org/10.1109/TIM.2008.2007041

## Disclaimer

Certain commercial equipment, instruments or materials are identified in this paper in order to adequately specify the environmental and experimental procedures. Such identification does not imply recommendation or endorsement by the BIPM or PTB, nor does it imply that the materials or equipment identified are necessarily the best available for the purpose.

## Appendix A

This appendix describes additional measurements and analyses performed.

### A1: Gain error evaluation

As reported above, the gains of the two 5922 samplers were regularly calibrated before the ABBA series. Figure A1 shows the changes in the gain compared to the value measured directly beforehand for the days of the comparison. The BIPM sampler is more stable, and its gain varies less. In addition, the values for both samplers appear to stabilize after 3 days.

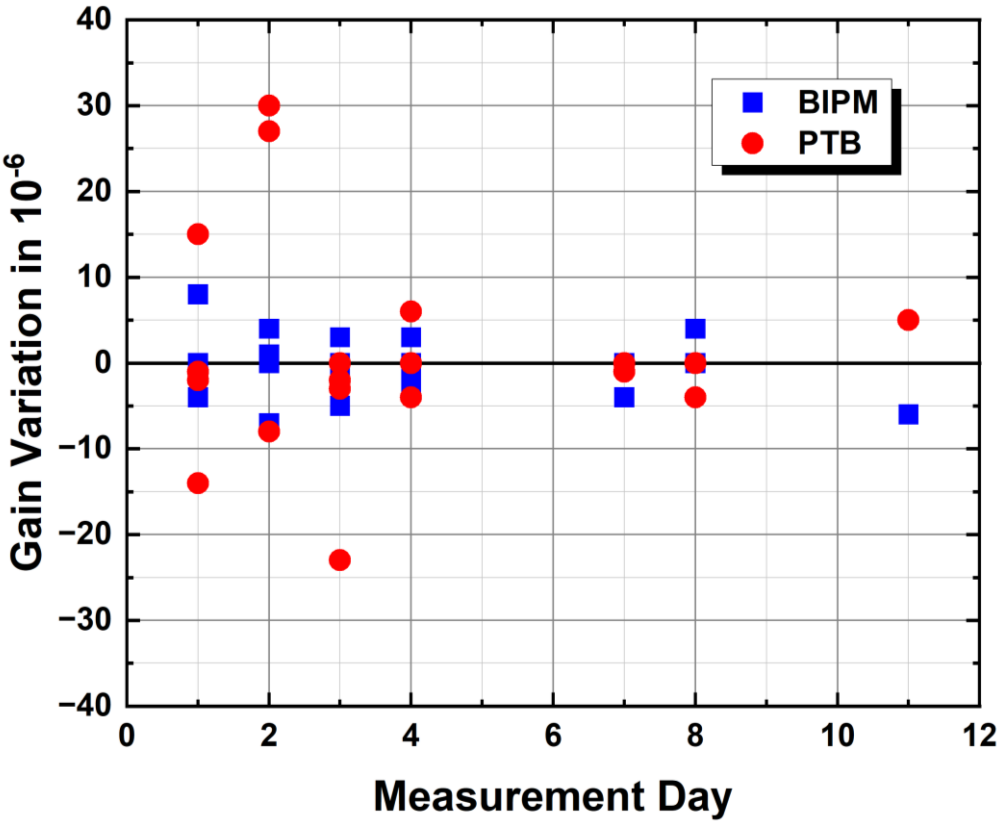


**Fig. A1**: Gain variation from one ABBA measurement series to the next.

Based on this variation we estimated the Type B uncertainties as shown in tables 1 and 2. Gain variations during an ABBA series contribute to the Type A uncertainty.

**A2: Cable error**

The cable error was determined by extending the cables by 1 m and 2 m on both Josephson voltage outputs. Comparative values without extension (0 m) were taken at the beginning and end of the measurements. These were then averaged and compared with the other values. Figure A2 shows the relative deviations in parts in $10^8$. The changes for the two cable extensions were then fitted using a square law to determine the difference to 0 m. This results in a cable error estimation of approximately $2 \times 10^{-9}$ at 1 kHz. This error depends on the square of the measured frequency, but not on the measured voltage.

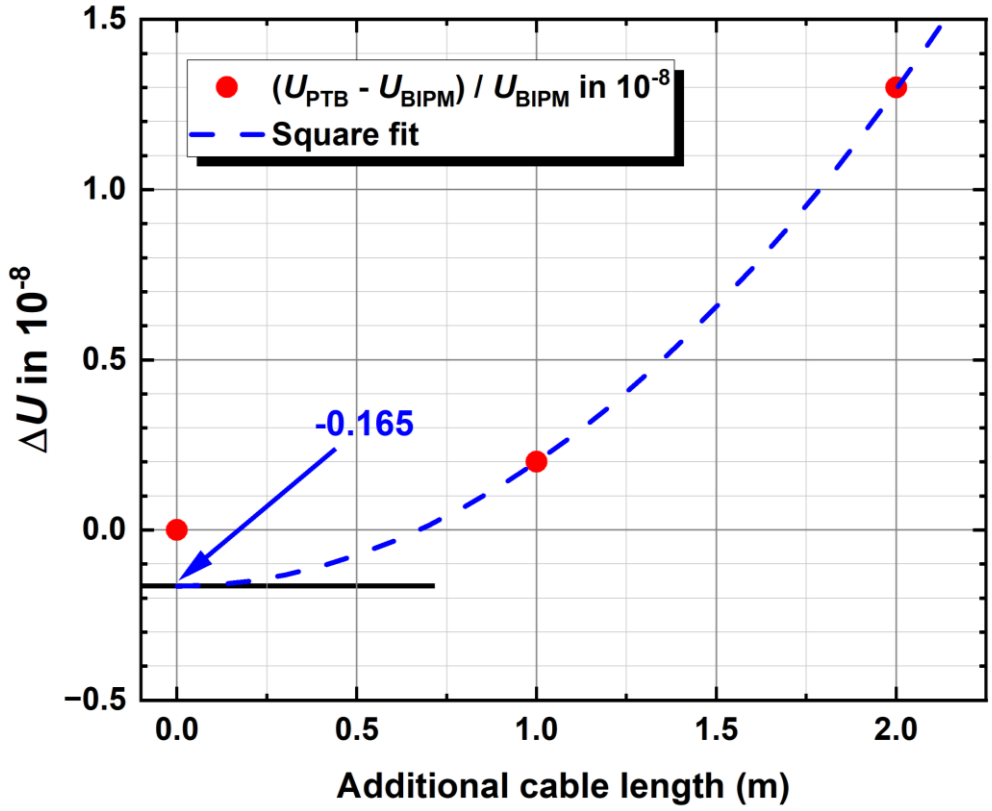


**Fig. A2**: Measurements with additional cable lengths 1 m and 2 m, respectively. A quadratic fit indicates a possible cable error for the comparison.

### A3: Typical tracing of the SWG output voltage

The ability to carry out the measurements in quick succession meant that the output voltage of the SWG could be tracked very well. An example of this is shown by the individual measurements in a complete ABBA sequence in Fig. A3. The output voltage of the SWG was only unstable in the morning after switching on and after modifications to the module, which led to temperature changes of several kelvin, for example. Fig. A4 shows how stable the SWG was after a longer run-in phase.

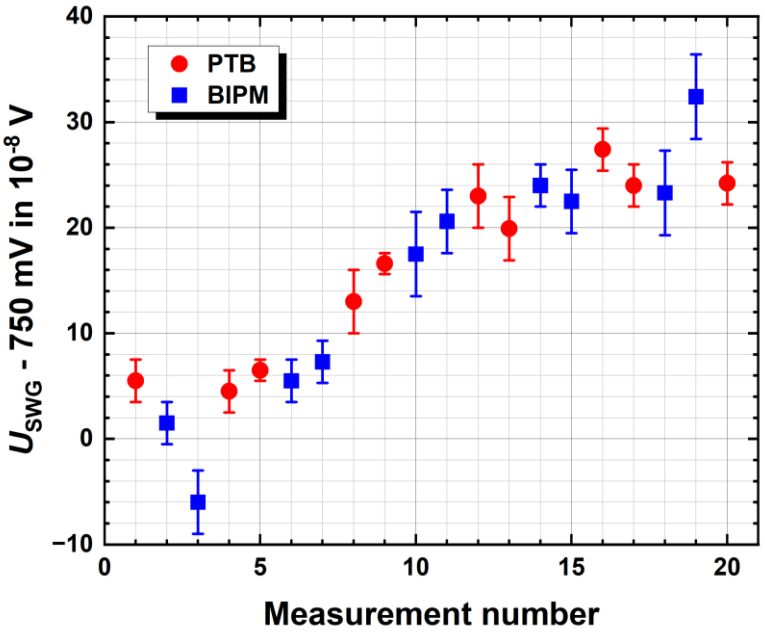


**Fig. A3**: Tracking the output voltage of the SWG with both AC quantum voltmeters.

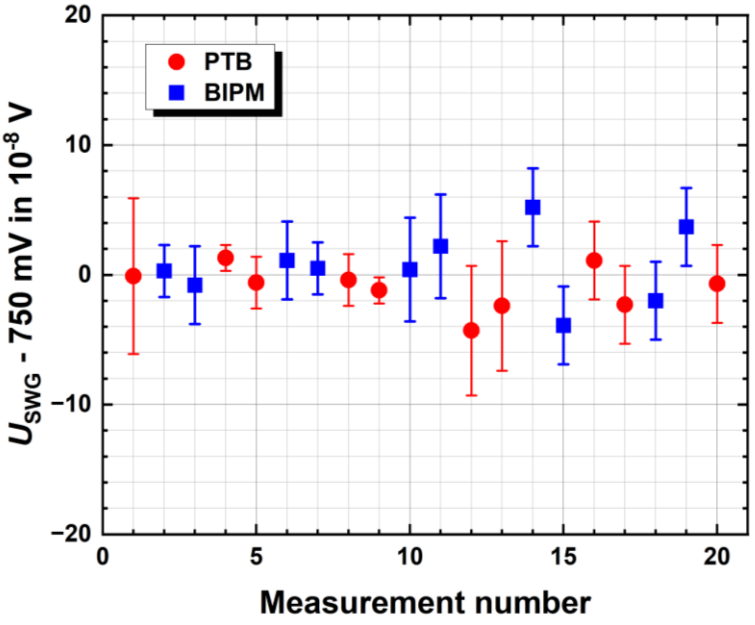


**Fig. A4**: Measurements of the SWG voltage after a running-in phase.

### A4: Typical Allan deviation

Figures A5 and A6 show selected Allan deviation analysis curves for frequencies 62.5 Hz, 312.5 Hz and 1 kHz at the two voltage levels 0.75 V and 7 V. Please note that these are absolute values. It is easy to see that the deviation for all measurements follows a white noise behavior up to 60 s very well. Measurement uncertainties of $2 \times 10^{-8}$ V are typically achieved for those times.

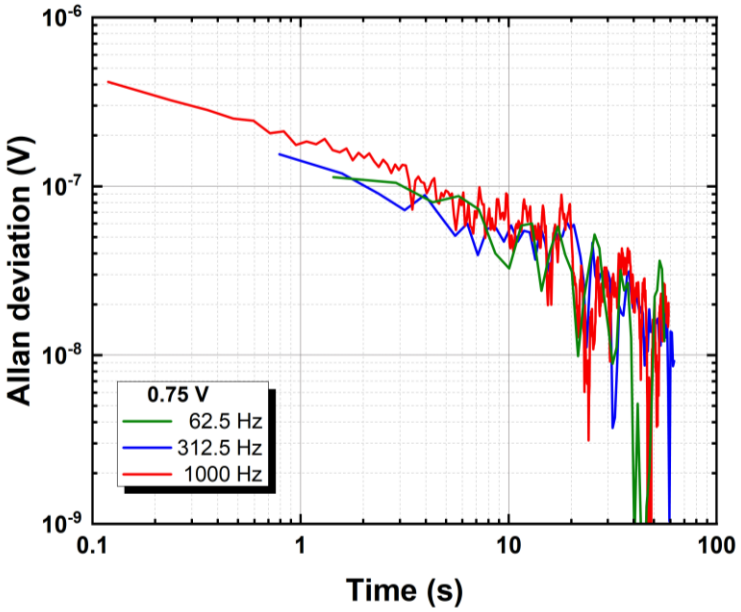


**Fig. A5**: Allan deviation analysis for measurements at different frequencies at 0.75 V.

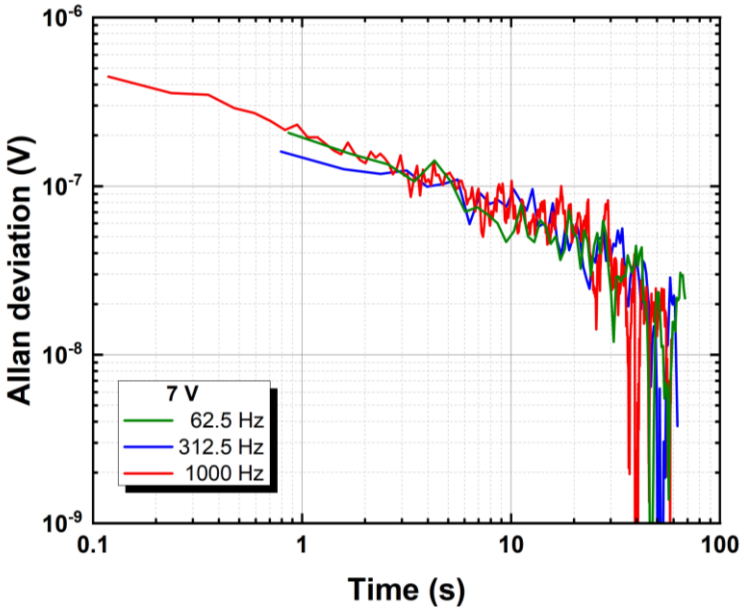


**Fig. A6**: Allan deviation analysis for measurements at different frequencies at 7 V.

### A5: Error due to the switch

The error contribution from the switch was evaluated experimentally by performing two consecutive measurement series immediately before (*Forward*, full symbols) and after (*Reversed*, open symbols) interchanging the inputs used by the two AC quantum voltmeters. Fig. A7 shows the four results related to a reference voltage for BIPM and for PTB at 0.75 V and 1 kHz. The differences between *Forward* and *Reversed* measurements were $-0.7 \times 10^{-8}$ V and $3.2 \times 10^{-8}$ V for the BIPM and PTB, respectively. From this we estimate the relative Type B error to be $((3.2 - 0.7) / 2) \times 10^{-8}$ V / $\sqrt{2}$ / 0.75 V = $1.2 \times 10^{-8}$ V V$^{-1}$ ($k$ = 1).

Such a systematic error is most likely caused by the slightly different electronic components in the switch, which lead to runtime differences between the two outputs. Therefore, the Type B relative error for 7 V is just as large.

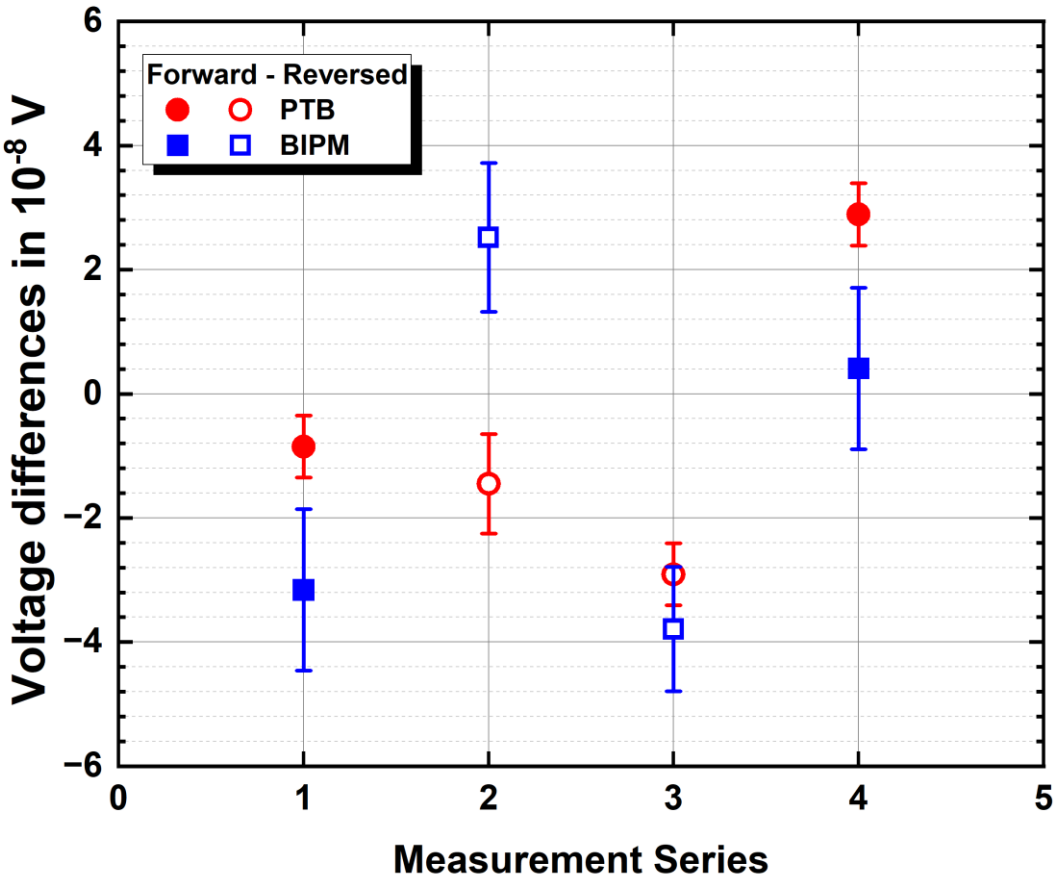


**Fig. A7**: Results of series measurements before and after interchanging the inputs from the switch to the two AC quantum voltmeters at 0.75 V RMS (*Forward*, full symbols and *reversed*, open symbols). The error bars indicate the standard deviation of the mean for each series for $k$ = 1.

**A6: CMRR error of PXI NI 5922**

Following the measurements, the common mode rejection ratio was measured for one sampler. Fig. A8 shows the measured values in red and dB (right axis). As the sampler was only used at 7 V on 'high', a systematic measurement error can be calculated directly from this. This CMRR error is shown in Fig. A8 with the black values (left axis). During the comparison at 7 V both AC quantum voltmeters were operated in the same way i.e. sampler on 'high'. If we also assume that the CMRRs of the two samplers differ by a maximum of 10 % (rectangular distribution), then these frequency-dependent errors are largely cancelled out. The remaining Type B error at 1 kHz is listed in table 2.

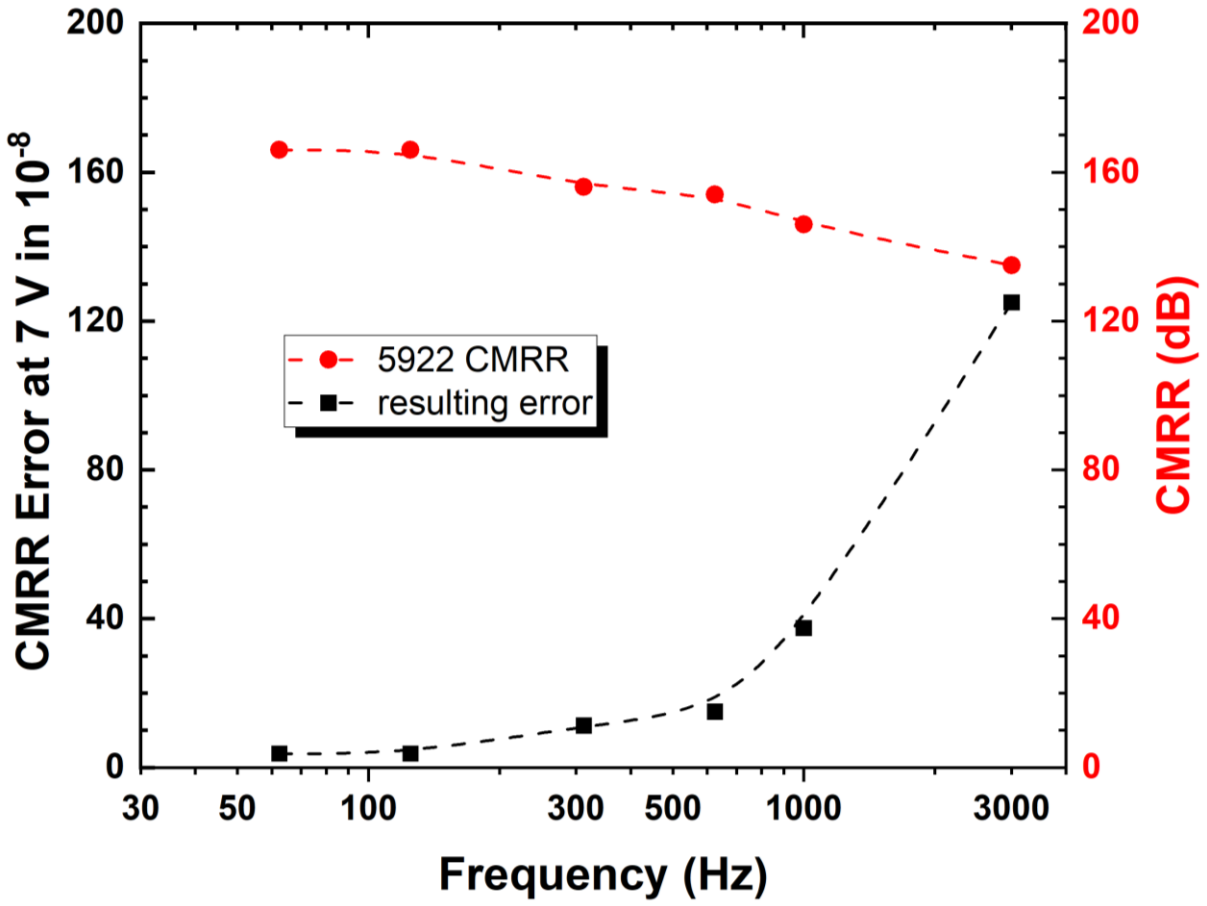


**Fig. A8**: CMRR for the NI5922 sampler as function of frequency (right axis). The resulting measurement error at an amplitude of 7 V is shown with the black dots (left axis).